




Theses and Dissertations

2010-07-14

An Experimental Investigation of Friction Bit Joining in AZ31 Magnesium and Advanced High-Strength Automotive Sheet Steel

Rebecca Gardner
Brigham Young University - Provo

Follow this and additional works at: <https://scholarsarchive.byu.edu/etd>

 Part of the [Construction Engineering and Management Commons](#), [Manufacturing Commons](#), and the [Mechanics of Materials Commons](#)

BYU ScholarsArchive Citation

Gardner, Rebecca, "An Experimental Investigation of Friction Bit Joining in AZ31 Magnesium and Advanced High-Strength Automotive Sheet Steel" (2010). *Theses and Dissertations*. 2159.
<https://scholarsarchive.byu.edu/etd/2159>

This Thesis is brought to you for free and open access by BYU ScholarsArchive. It has been accepted for inclusion in Theses and Dissertations by an authorized administrator of BYU ScholarsArchive. For more information, please contact scholarsarchive@byu.edu, ellen_amatangelo@byu.edu.

An Experimental Investigation of Friction Bit Joining of
AZ31 Magnesium and Advanced High-Strength
Automotive Sheet Steel

Rebecca Gardner

A thesis submitted to the faculty of
Brigham Young University
in partial fulfillment of the requirements for the degree of
Master of Science

Mike Miles, Chair
Kent Kohkonen
Perry Carter

School of Technology
Brigham Young University

August 2010

Copyright © 2010 Rebecca Gardner

All Rights Reserved

ABSTRACT

An Experimental Investigation of Friction Bit Joining of AZ31 Magnesium and Advanced High-Strength Automotive Sheet Steel

Rebecca Gardner

Master of Science

Friction Bit Joining (FBJ) is a recently developed spot joining technology capable of joining dissimilar metals. A consumable bit cuts through the upper layer of metal to be joined, then friction welds to the lower layer. The bit then snaps off, leaving a flange. This research focuses on FBJ using DP980 or DP590 steel as the lower layer, AZ31 magnesium alloy as the top layer, and 4140 or 4130 steel as the bit material.

In order to determine optimal settings for the magnesium/steel joints, experimentation was performed using a purpose-built computer controlled welding machine, varying factors such as rotational speeds, plunge speed, cutting and welding depths, and dwell times. It was determined that, when using 1.6 mm thick coupons, maximum joint strengths would be obtained at a 2.03 mm cutting depth, 3.30 mm welding depth, and 2500 RPM welding speed. At these levels, the weld is stronger than the magnesium alloy, resulting in failure in the AZ31 rather than in the FBJ joint in lap shear testing.

Keywords: Rebecca Gardner, FBJ, friction bit joining, spot joining, dissimilar metals, magnesium, high strength steel

Table of Contents

List of Tables	v
List of Figures	vi
Chapter 1	1
1.1 Introduction.....	1
1.2 Motivation for work.....	1
1.3 Hypotheses.....	2
1.4 Methodology summary	2
1.5 Delimitations and assumptions	3
Chapter 2. Review of literature	5
2.1 Introduction to literature	5
2.1 Prior work	5
2.2. Competitive technology	6
2.3 Related technology.....	7
2.4. Problems in related technologies	9
Chapter 3. Methodology	11
3.1 Process description.....	11
3.2 Generation of data.....	17
Chapter 4. Results and analysis	19
4.1 Initial experiments	19

4.2 Replication of previous DOE.....	20
4.3 Bit programming improvement.....	23
4.4 “Fast cycle” experiment.....	24
4.5 Cross-tension and t-peel.....	28
4.6 Depth study.....	30
4.7 DOE.....	33
Chapter 5. Conclusions.....	36
5.1 Summary of work.....	36
5.2 Conclusions.....	36
5.3 Recommendations.....	37
References.....	39
Appendix A Glossary of terms.....	41
Appendix B Machine code for fluted bits.....	44
Appendix C DOE recorded data.....	46
Appendix D DOE analysis.....	50

List of Tables

Table 1 Blank observation table	14
Table 2 Codes and definitions.....	16
Table 3. Current functional parameters	17
Table 4 Initial parameters	20
Table 5 DOE replication levels.....	21
Table 6 Results of partially replicated DOE.....	22
Table 7 Fast cycle parameters.....	24
Table 8 Fast cycle results with DP 590.....	24
Table 9 Fast cycle with DP 980	26
Table 10 Settings without weld dwell.....	27
Table 11 Results without weld dwell.....	27
Table 12 Depth study parameters	31
Table 13 Depth study data	31
Table 14 DOE factor levels.....	34
Table 15 DOE parameters.....	34

List of Figures

Figure 1 FBJ welding machine, shown.....	4
Figure 2. Fluted and flat FBJ bits.....	11
Figure 3 Coupons set up in preparation for joining	12
Figure 4. Welded and marked samples, ready for lap shear strength testing.....	14
Figure 5 "Good" joint (shown with aluminum/steel sample)	15
Figure 6 "No-flange" joint	15
Figure 7 Fracture in weld.....	16
Figure 8 Fracture in Mg	17
Figure 9 Configurations, left to right: lap shear, t-peel, cross-tension	18
Figure 10 Lap shear sample configuration.....	19
Figure 11 Fluted bits	23
Figure 12 DP 590 fast cycle strength results	25
Figure 13 DP 980 fast cycle strengths	26
Figure 14 Strengths without weld dwell.....	28
Figure 15 a) cross-tension, b) t-peel	29
Figure 16 Cross tension results.....	29
Figure 17 T-peel results	30
Figure 18 Sample A, nominal welding depth 3.3 mm	32
Figure 19 Sample B, nominal welding depth 3.56 mm	32
Figure 20 Sample C, nominal welding depth 3.81 mm	33
Figure 21 Pareto chart with significance calculated at $\alpha=.01$	35

Chapter 1

1.1 Introduction

Friction Bit Joining (FBJ) is a recently developed spot joining method applicable to dissimilar metals. Comparable in usage to other spot joining technologies, such as Resistance Spot Welding (RSW), Friction Stir Spot Welding (FSSW) and Self-Piercing Riveting (SPR), FBJ has greater potential for use with a wide variety of materials. These terms and others are defined in Appendix A. FBJ is a solid state process like FSSW, but uses a consumable bit, as does SPR. Previous work on this technology has been performed by professors and students at Brigham Young University, with emphasis on steel-to-steel and steel to aluminum joints. More on this will be discussed later.

1.2 Motivation for work

For over a decade, it has been clear that reducing the weight of vehicles is a necessity in the automotive industry (Cole and Sherman 1995). At first a necessity in order to improve mileage in gasoline-powered vehicles, the need to reduce weight has come to be of greater importance with the introduction of electric and hybrid vehicles and other alternative fuel vehicles. In these vehicles, additional weight is often added by large battery cells or other necessary components, so the reduction in chassis weight becomes key to the mileage and speed achievable.

One solution to the weight problem is the introduction of lighter metals into the vehicle design. These metals can include aluminum alloys, magnesium alloys, and high strength steels. Unfortunately, these alloys are not as easily formed or joined in production settings as their predecessors. Therefore, a process which allows various components--each made from whichever material is most suited to its size and function—to be joined together in a rapid and strong manner, will be beneficial to the automotive industry and potentially to other industries as well.

1.3 Hypotheses

This work will focus on the use of FBJ to join magnesium to steel. In order to evaluate the usefulness of the technology, the following hypotheses will be tested:

1. The FBJ process can successfully join magnesium alloys to steel alloys with a lap shear strength in excess of 4448 N, using Self Piercing Riveting (SPR) as a benchmark for comparison.
2. The FBJ process time for joining magnesium alloys to steel alloys will be 2 seconds or less.

1.4 Methodology summary

Friction Bit Joining is performed using a consumable bit with an integrated cutting edge. The bit should be made of a metal capable of joining to the substrate layer using traditional rotational friction welding. Essentially, the bit cuts through the top layer, wearing down the cutting edge as it goes. The remaining bit surface then friction welds to the substrate layer.

After a brief cooling period, the bit is snapped off, leaving a flange joining the top layer to the lower sheet.

In order to test the hypothesis and determine optimum operating parameters, it was first necessary to determine functional parameters which reliably give good welds. Using these parameters as a baseline, further experimentation using Design of Experiments (DOE) techniques allowed a range of variables to be simultaneously tested. Through an iterative process, optimal parameters have been identified.

1.5 Delimitations and assumptions

FBJ has the potential to be used for a wide variety of metals. Current research by this researcher and others involves joining of steel alloys, aluminums, and magnesium, with many different combinations, such as magnesium to aluminum and magnesium to magnesium. However, this work will specifically address the joining of magnesium to steel. Experimentation with other combinations will proceed concurrently, and discoveries in those areas may prove beneficial to the magnesium-to-steel research. The scope of this particular study will be limited to friction bit joining of magnesium to steel using steel bits.

Another benefit of FBJ is the potential to be applied to a variety of thicknesses of metal, according to the bit design. In order to keep the scope of this work at a practical level, this study has been limited to sheet metals approximately 1.6 mm in thickness. Also, in the interests of standardization, the samples used for experimentation are coupons 25 mm x 100 mm for the lap shear and t-peel testing, and 50 mm x 250 mm for cross-tension testing.

Joint strengths were tested on the Instron Tensile Test machine located in the research lab. This machine has been appropriately calibrated and it is assumed that, with correct set-up

and operating procedures, the resulting data is accurate. Likewise, it is assumed that the read-out data from the purpose-built welding machine (see Figure 1) is also accurate and reliable.



Figure 1 FBJ welding machine, shown without stiffness reinforcement

Chapter 2. Review of literature

2.1 Introduction to literature

Limited literature is currently available pertaining directly to the newly developed Friction Bit Joining (FBJ) process. However, a multitude of information is present on related technologies. The related technologies include those that may be considered competitive in purpose, such as Self Piercing Riveting (SPR), a purely mechanical method capable of joining dissimilar metals, and clinching. Also of interest are welding methods which are related by means of similarity to the welding in the FBJ process, such as the various friction welding processes, and those that, though very different, yield information that may be pertinent, such as laser welding. Problems which have arisen when welding with the aforementioned processes are also likely to arise in the FBJ process, and the findings of the researchers in these related fields can help guide the FBJ researcher to solutions to the same problems.

2.1 Prior work

One prior paper on FBJ technology is “Solid state spot joining of sheet materials using consumable bit” (Miles, et al. 2009). This article discusses experiments performed on Ultra High Strength Steel (UHSS) and an aluminum alloy. UHSS/UHSS joint strengths were compared to results of resistance Spot Welded (RSW) joints. FBJ joints are found to give satisfactory results, although the process was considered too slow for production. However, FBJ

is shown to be usable for materials and material combinations that do not give satisfactory results using RSW or Self Piercing Riveting (SPR).

2.2. Competitive technology

Currently, the likely technology for joining such dissimilar metals as magnesium and steel is SPR. SPR is a mechanical joining method, and thus is not as heavily restricted by materials as welding technologies are. However, the thickness of materials is a restriction with SPR; less than 6 mm of total joint thickness for steel and 10 mm for lighter weight alloys. The process of SPR is fairly simple. A punch first presses the rivet against the materials to be joined, clamping against the underlying die. The punch then pushes the rivet through the top layer (piercing, rather than riveting through pre-drilled holes). The last step of the joining process is flaring, which involves the material of the lower layer flowing into the die, which also flares the rivet out, mechanically interlocking the rivet in the lower metal and firmly holding the top layer in place. (He, Pearson and Young 2008) Research into SPR failure modes (when joining aluminum samples) has revealed that fretting can occur in the interface between the rivet and metals being joined (Chen, et al. n.d.) and that, in fatigue testing, the joint is most likely to fail either by means of rivet pull-out or cracking of the top layer in the vicinity of the rivet (Fu and Mallick 2003). Strengths vary depending on the design of the rivet and die, but in general, strength of SPR joints are comparable to or higher than resistance spot welded joints for these same materials (He, Pearson and Young 2008). That comparison, of course, is only applicable to those materials which can be successfully spot welded.

Clinching also joins overlapping sections using mechanical deformation. In the case of dieless clinching as described by Neugebauer (Neugebauer, Dietrich and Kraus 2007), a punch is

forced into the materials to be joined. The top layer is pressed into the bottom, flowing outward into the lower layer. This requires a certain level of formability, which is not easily attainable with magnesium. Neugebauer describes a few methods of heating the magnesium to overcome this, such as preheating the metal to be joined or clinching with a heated punch and anvil. This heating, to 220° C, is necessary to prevent cracking of the magnesium. Although continued experimentation has been done to reduce the time necessary for this heating, it is noteworthy to observe that FBJ has no such requirement in order to work with magnesium alloys.

2.3 Related technology

Welding processes for joining dissimilar metals, currently in use and in research, include Friction Welding (FW), Friction Stir Welding (FSW), Friction Stir Spot Welding (FSSW), and laser welding. FW joints are frequently butting configurations of round stock. FSW joints are generally performed on butted edges of sheet metal or plate. FSSW is performed on a lapping configuration of sheet stock, and laser welding, which can be used in many configurations, is also used for lapped joints.

FW consists of plunging a rapidly rotating member into a stationary member. The heat and force caused by the friction deforms the ends of the metals and causes a weld between them. No tool is used in creating the weld. In a study on friction welding of dissimilar stainless steels, the corrosion resistance, toughness, and strength of the welded area were shown to be better than that of the parent metals (Satyanarayana, Madhusudhan Reddy and Mohandas 2005). This is interesting to note, because a strong, successful rotational friction weld is necessary in FBJ.

FSW is not as directly related to FBJ, except that it has been shown to be useful in certain dissimilar metal applications. FSW consists of plunging a rapidly rotating, non-consumable tool

transversely between abutting metals. The rotation of the tool serves two purposes: first, to create frictional heat to soften the metals, and second, to intermingle the softened metals. A study on FSW joining of magnesium to aluminum showed that defect-free joints could be successfully formed, but that the strength of the weld was not significantly affected by the speed of rotation within the range tested, 1000 to 1400 rpm (Kwon, Shigematsu and Saito n.d.).

A related welding technology is FSSW. It is similar to FSW, but the materials to be joined are lapped, rather than butted. A similar non-consumable tool is used, but it is not moved transversely. Rather, it is plunged through the upper layer into the lower, stirs the metals at that one spot, then is retracted. This joining method leaves a divot in the shape of the tool pin in the final joint. This method, like other technologies for making lapped joints, can potentially be used in conjunction with adhesive bonding. Cured adhesive FSSW bonds of aluminum was shown in one study to have almost three times the lap shear strength of similar joints without adhesive (Pan, Schwartz and Lazarz n.d.). That study indicated that the adhesive was not found within the weld, only around it.

However, in FSSW joining of dissimilar magnesium alloys, problems have been found with cracking. In a study into this problem (Yamamoto, et al. 2008), it was found that the parameters of the weld, including the upper or lower positioning of the problematic materials, could control and reduce the problem. Cracking has also been found to be a problem in RSW joining of magnesium alloys. In one study, cracking in the weld nugget was found to begin when currents greater than 15 kA were used for the resistance weld (Sun, et al. 2007). The authors of that paper determined that the higher current, which resulted in higher weld temperatures, led to an increased tensile stress within the joint in cooling. The current research of Mg-UHSS FBJ joints involves the cutting of magnesium prior to the weld, but as additional

research is desired into the use of FBJ to join Mg to Mg, as well, the knowledge of how to control problems with welded magnesium alloys is needed.

Laser welding has been used for joining a variety of metals, including aluminum to magnesium and dissimilar magnesium alloys. In welding of butted dissimilar magnesium samples, tensile strengths of the welds are shown to be 90% or more of the strengths of the individual alloys (Quan and etal n.d.). The same study also found that the microhardness of the alloys decreases in the heat affected zones. This finding is also of interest to the researcher studying the FBJ process, because the top layer of the joint is exposed to the heat formed by the friction weld. Because the heat could detrimentally affect the material properties of the magnesium layer, it is desirable to keep the temperature and duration as low as possible, while still forming a good weld. Another concern with laser welding is the risk of burn-through. Some researchers have had success in reducing risk of burn-through by combining laser welding with gas tungsten arc welding for welding magnesium alloys (Song, Liming and Peichong 2006).

2.4. Problems in related technologies

In welds involving magnesium alloys and/or magnesium-rich aluminum alloys, a common problem is the formation of intermetallic layers that weaken the joint. For different types of welding, different solutions to the problem have been found.

In the case of laser-welded lap joints of magnesium to aluminum, the standard method of welding across the center of the lap was found to increase the intermetallic layer. When the researchers changed the weld position to along the ends of the lapped sections, they found that the shallower weld penetration depth yielded a smaller intermetallic layer (Borrisutthekul, Miyashita and Mutoh n.d.).

In a Japanese study of rotational friction welding of various aluminum alloys to carbon steel, the intermetallic layer was found to increase with increased pressure, longer friction time, and a larger number of rotations. This study also found that aluminum alloys with a high magnesium content formed greater intermetallic layers and that the weldability of the aluminum alloy to the steel decreases (Ochi, et al. 2004).

Chapter 3. Methodology

3.1 Process description

Friction Bit Joining is a multi-stage joining process. In the first stage, the top layer of the lapped joint is cut away in order to expose the bottom layer where friction welding will take place. This can be done with either fluted or unfluted cutting geometry. Fluted bits have channels cut behind the cutting edges (see Figure 2).

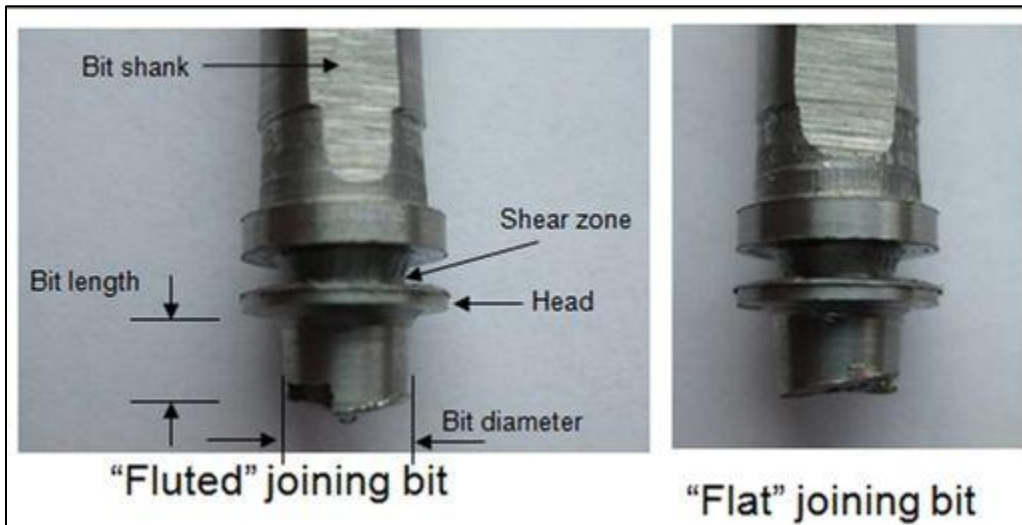


Figure 2. Fluted and flat FBJ bits

These channels, or flutes, allow for the clearing out of chips generated while cutting, but reduce the surface area for welding and could possibly result in voids in the interface, weakening the joint. Next, the RPM of the bit is increased in order to create heat to form a friction weld

between the bit and lower layer. At this point, rotation ceases and pressure continues to be applied for a brief cooling time. Finally, rotation begins again and the chuck is retracted, resulting in a break between the flanges. All of the RPMs, plunge rates, plunge depths, and times are controlled by a computer integrated with the purpose-built welding machine. Bits are machined from 3/8" round stock. For these experiments, 4140 steel was used. For other sheet metal combinations, heat treating the bits is necessary. However, thus far it does not appear to add an advantage to Mg-steel FBJ joints. A set-up in the welding machine is shown in Figure 3.

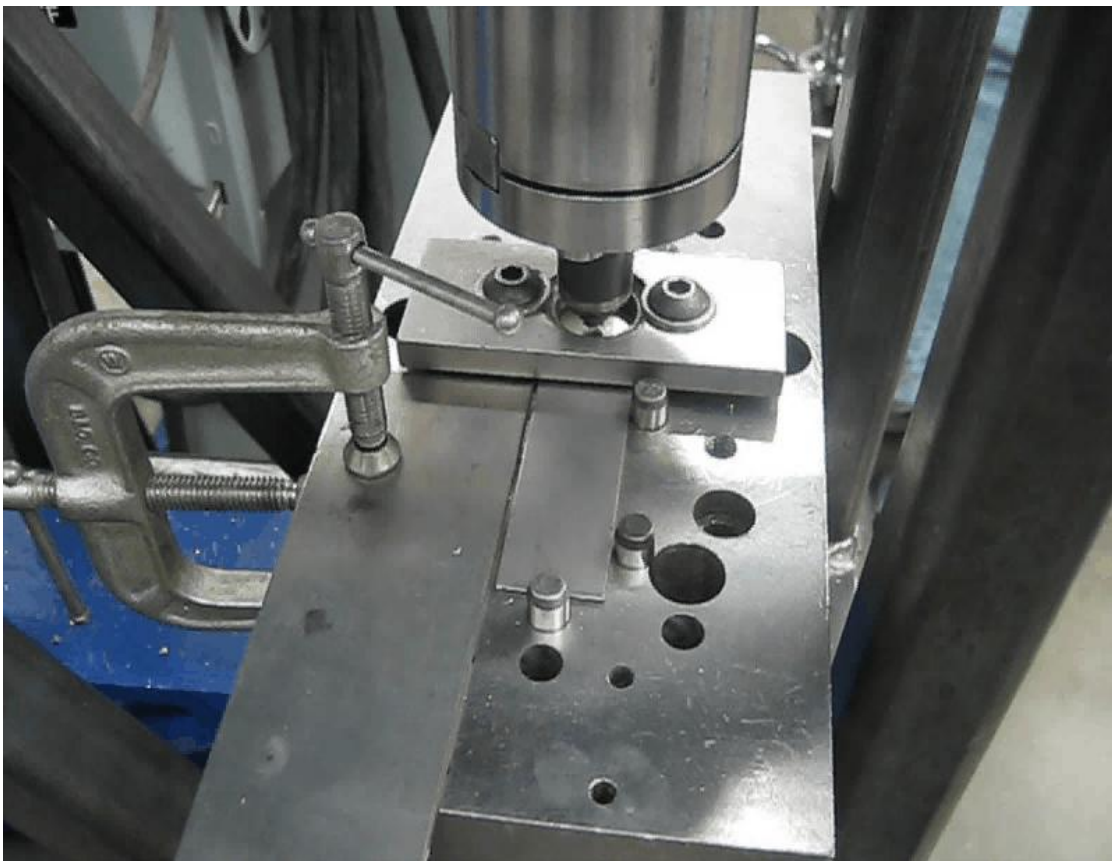


Figure 3 Coupons set up in preparation for joining

Bits were machined on an Okuma CNC lathe with live tooling, which was necessary for producing the cutting edges and flutes. A gauge was used to make sure the proper length of stock was extended from the chuck. Shank diameter of completed bits was monitored, as tool wear would result in larger diameters which would not fit in the tool holder on the welding machine. Tool offsets were adjusted as necessary to keep dimensions in tolerance. After machining the bits, some handwork was necessary; a flat was ground on one side of the shank for set screw in the tool holder, and burs on the cutting edges were filed off.

For experiments, the following procedure is followed:

1. Samples cut to 25x100 mm coupons using manual shear
2. Steel bits cut from 4140 round stock, not heat treated, Rc hardness about 28-30
3. Coupons clamped in position on welder, steel as bottom layer, magnesium alloy on top
4. Bit tightly fastened in with set screw against ground flat
5. Cycle parameters entered in control computer
6. Tool length touch-off performed
7. Run cycle
8. Record force and depth
9. Remove sample, label (see Figure 4)
10. Position sample in Instron (with shims to keep sample aligned correctly for shear testing)
11. Pull at 10 mm/min
12. Record peak load

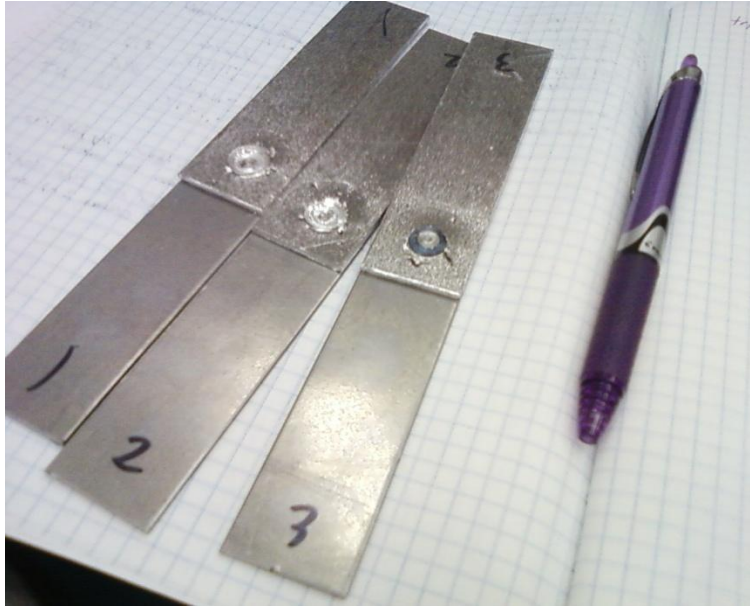


Figure 4. Welded and marked samples, ready for lap shear strength testing

A simple table was used for recording data and observations. This table includes columns for data taken from the welding machine readout at the conclusion of the welding cycle (maximum force and maximum depth), a column for the peak load observed when the lap shear samples were pulled in the Instron machine, a code to briefly describe the quality of the joint (noted prior to testing), and any other comments, which include information such as failure mode or any other observations that seem worth noting. See Table 1 for an example.

Table 1 Blank observation table

Run Order	Max force	Max depth	Shear force	Code	Comments
1					
2					
3					
4					
5					

The codes in the observation table refer only to the visual observation of the joint. A correctly formed joint, where the bit welded to the lower layer and broke between the two flanges, was considered “Good”, as shown in Figure 5.

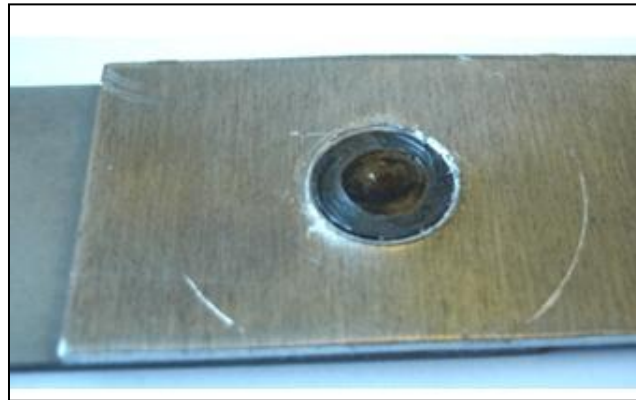


Figure 5 "Good" joint (shown with aluminum/steel sample)

At times the bit may have welded fully or partially to the lower layer so that the two layers were held together, but the flange was not left intact when the bit broke. This type of joint was identified as “No Flange”. An example is shown in Figure 6.



Figure 6 "No-flange" joint

If the welding cycle did not cause the two layers to be held together at all (or the joint was so weak that it broke during removal from the welding fixture or when being inserted in the clamps for testing in the Instron), it was considered “No Join”. The codes used to indicate these terms are shown in Table 2.

Table 2 Codes and definitions

Code	Definition
G	Good
NF	No Flange
NJ	No Join

The “Comments” column in the observation table was used for recording other information of interest, such as notes on failure modes. Three primary failure modes have been observed in FBJ research:

1. Pull-out, where the upper layer of the sample pulls free of the bit flange without breaking the weld. This mode has not been observed in lap-shear testing of Mg/Steel joints.

2. Fracture in weld, where the break occurs at the interface between the lower coupon and the bit. See Figure 7.



Figure 7 Fracture in weld

3. Fracture in the upper coupon. This is most common where the upper layer has a lower shear strength than the friction weld, such as in the Mg/Steel joints. See Figure 8.



Figure 8 Fracture in Mg

3.2 Generation of data

The data of interest to this research include the various input parameters as well as the output variables of joint strength, and welding force and measured depth (force was collected by a sensor under the welding area; depth was measured by a laser micrometer on the head of the welding machine). The initial parameters were based on trial and error, previous work, and educated guesses. When a promising set of parameters were determined (see Table 3), a series of at least five samples were run at the same settings for confirmation of the strength of the joint.

Table 3. Current functional parameters

Cycle Segment	Cutting	Welding	Cooling
RPM	1200	2160	0
Plunge Rate (in/min)	10	10	0
Depth (in)	-0.09	-0.14	-0.14
Dwell (ms)	0	500	500

Using parameters thus generated as a baseline, a designed experiment was planned and executed. For ease of design, testing variables at two levels is preferred. However, including a third center-point level increases the chances of the researcher being able to detect non-linear response curves. This is an iterative process, where each set of experiments lead to another, until a response curve or equation can be identified, which will result in the optimum parameters. This was the methodology used to test the strength hypothesis. In addition to the lap-shear testing previously described, other joint configurations were made and tested: T-peel and cross-tension. (See Figure 9) Select samples were cut, mounted, and polished for analysis rather than pulled to failure for strength testing.

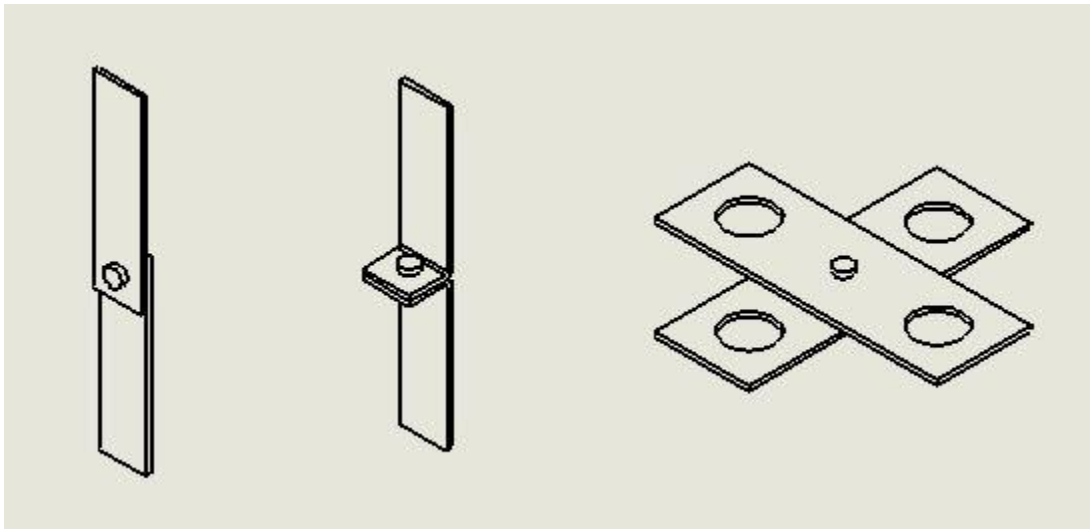


Figure 9 Configurations, left to right: lap shear, t-peel, cross-tension

Chapter 4. Results and analysis

4.1 Initial experiments

Prior research on Friction Bit Joining focused largely on steel-to-steel and aluminum-to-steel joints. However, some exploratory work was done on other metals and configurations, including magnesium alloy-to-steel. It should be noted that when no other sample configuration is specified, the samples tested were lap shear sample, as illustrated in Figure 10.

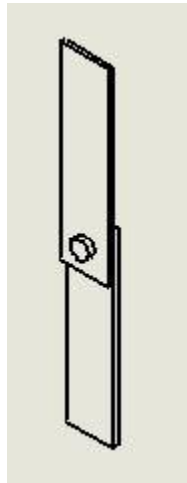


Figure 10 Lap shear sample configuration

The parameters used for that prior exploratory work were used for the initial experimentation in this research, as shown in Table 4.

Table 4 Initial parameters

	Cutting	Welding	Cooling	Break bit
Stage	1	2	3	4
RPM	700	1800	0	700
Plunge rate (mm/s)	1.27	1.27	0.00	4.23
plunge depth (mm)	-3.05	-4.06	-4.06	5.08
Peck cycles	1	0	0	0
dwell (ms)	0	500	500	0

However, when a few bits were run at these settings in order to form a baseline for comparison, none of them successfully welded to the steel. It is assumed that between when exploratory studies were done by prior researchers and when this research was started, other factors may have been changed and not noted which caused the failure.

4.2 Replication of previous DOE

In order to develop a welding process for mg/steel joints, it was decided that a designed experiment (DOE) performed on FBJ joining of aluminum to steel be replicated, with the only change being that the top layer was magnesium alloy rather than aluminum. It was judged to be likely that the factors from that previous screening study that were significant for aluminum/steel joints could also be significant for Mg/steel joints, although the optimum levels would likely not be the same.

The factors in this experiment were bit length, weld time, and cool time, with the levels as shown in Table 5.

Table 5 DOE replication levels

Level	Length (mm)	Weld time (ms)	Cool time (ms)
-	4.445	500	500
0	5.207	1000	1250
+	5.969	1500	1500

This experiment was performed with unfluted bits. These bits have cutting edges machined into the end of the bits, but no flutes (channels for chip removal) cut into the sides. This design allows for greater surface area of the weld interface, as the complete face of the bit is available for bonding. The results are included as Table 6, but the full experiment was not completed due to the fact that too many samples failed to give good welds.

As the lap shear strength of the joint is the outcome to be evaluated, the high failure rate meant that statistical analysis could not be performed. Therefore, the experiment was halted before too many bits and coupons were wasted. However, observation of the failed joints revealed that the magnesium chips were melting and pooling between the coupons. This indicated that the fluted bit design (explained in Section 3.1), which could more efficiently clear chips from the weld location, would probably yield better joints. Using fluted bits (as shown in Figure 11) would decrease the surface area available for welding, but this loss is negligible compared to the lack of welding caused by a layer of melted magnesium between the steel bit and steel coupon.

Table 6 Results of partially replicated DOE

Run Order	Length	Weld time	Cool time	Z force max (N)	Z distance max (mm)	Lap shear (N)	Comments
1	-1	1	1	18095.3671	-4.27	3665.33	NF
2	0	0	0	17170.1369	-3.74	3705.37	NF
3	1	-1	-1	20217.169	-3.74	35372.26	NF
4	1	-1	1	6707.91878	-2.98	-----	NJ
5	1	1	-1	16707.5218	-3.55	3015.89	NF
6	0	0	0	13380.2518	-3.06	-----	NJ
7	-1	-1	-1	12027.9923	-3.44	5030.94	G
8	0	0	0	20693.1287	-4.27	3456.27	NF
9	-1	-1	1	17321.3765	-3.39	5635.90	G
10	1	1	1	18211.0209	-3.81	2668.93	NF
11	-1	1	-1	19029.4937	-4.08	3852.16	NF
1	-1	1	-1	14759.2006	-3.18		G
2	-1	-1	-1	8198.07315	-3.01		NJ
3	-1	1	1	15137.2995	-3.04		NF
4	0	0	0	18873.8059	-3.65		NF
5	1	1	1	18308.8818	-4.07		NF
6	1	-1	-1	14496.7555	-3.32		
7	0	0	0				
8	-1	-1	1				
9	0	0	0				
10	1	1	-1				
11	1	-1	1				
1	-1	-1	-1				
2	1	-1	-1				
3	-1	-1	1				
4	1	-1	1				
5	-1	1	-1				
6	1	1	-1				
7	-1	1	1				
8	1	1	1				
9	0	0	0				
10	0	0	0				
11	0	0	0				



Figure 11 Fluted bits

4.3 Bit programming improvement

Some changes were found to be necessary in the CNC program used to make the fluted bits. In the original program, the flutes were cut before the cutting edges. This resulted in a large bur of steel covering the flutes. This metal had to be removed in order for the flutes to be effective at clearing the chips. For research using heat treated bits, this was not a problem, because the thin bur became brittle in treatment and was easily removed before use. However, for this research, without heat treatment, the burs were more difficult to remove cleanly. Therefore, sections of code in the CNC program were rearranged in order to put the flute milling cycle after the cutting edges were created. This greatly reduced the amount of post-machining handwork required before the bits could be used. The revised machine code is included as Appendix B.

4.4 “Fast cycle” experiment

After some improvements to the program for cutting the bits (the primary change being changing the order of cuts so that the flutes are cut after the cutting edges), the next step was to return to finding working parameters to use as a reliable basis for experimentation. The settings shown in Table 7 were found to be promising and were evaluated in a small test of five samples.

Table 7 Fast cycle parameters

	Cutting	Welding	Cooling
RPM	1200	2160	0
Plunge (mm/s)	4.23	4.23	0
Depth (mm)	-2.29	-3.56	-3.56
Dwell (ms)	0	500	500

These settings were found to give reliable results when used with a fluted bit and a DP 590 substrate, as shown in Table 8.

Table 8 Fast cycle results with DP 590

Run Order	Max force	Max Depth (mm)	Shear force (N)	Code	Comments
1	17908.54	-4.77	5253.35	G	Flange popped off when pulling sample
2	18166.54	-4.67	5400.14	G	bit broke
3	19807.93	-4.50	5159.94	G	bit broke
4	19372.01	-4.71	5102.11	G	bit broke
5	18313.33	-4.43	5426.83	G	bit broke

The series of five samples run at identical settings resulted in an average joint shear strength of 5268 N, with a standard deviation of 143 N. This was quite satisfactory, meaning

that these settings and bit design could be used as the basis for the rest of the study. Figure 12 shows the strengths of the five samples visually.

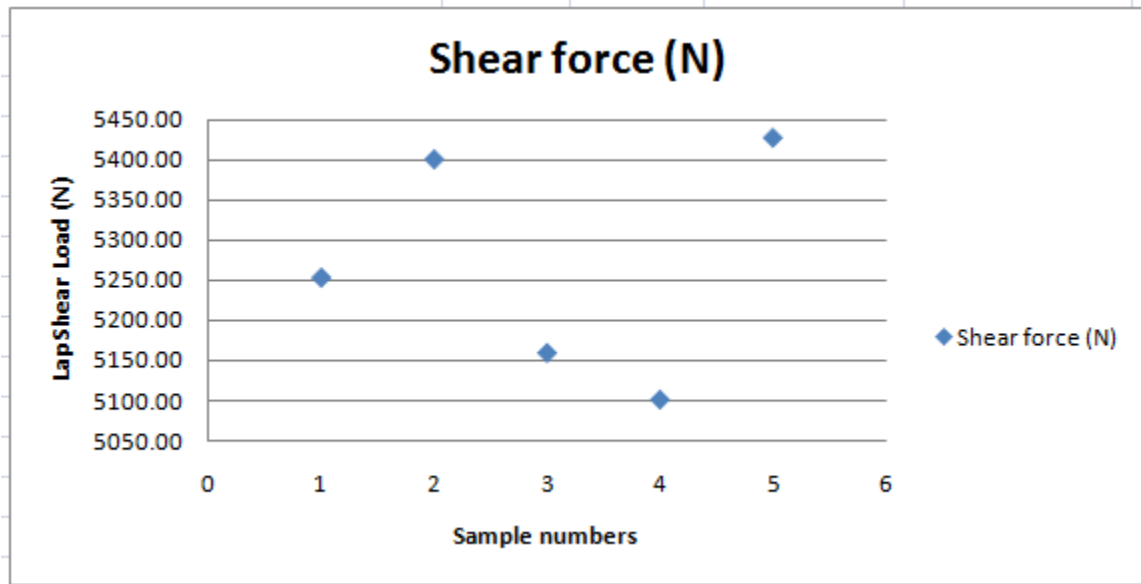


Figure 12 DP 590 fast cycle strength results

Later, the same “fast cycle” settings were tested using DP980 steel as the substrate, with results as shown in Table 9. The welding machine gave an erroneous reading of the maximum depth for sample 1. However, as the weld was good and the rest of the data seems reasonable, this point was not discarded and re-done. Likewise, as there was no obvious cause for the lack of a flange on the joint for sample 4, that data point could not be discarded as being erratic.

Table 9 Fast cycle with DP 980

Run order	Max force (N)	Max depth (mm)	Shear strength (N)	Code
1	25154.69541	-86.36	5529.139946	G
2	23362.06194	-4.953	5088.765968	G
3	23900.29681	-5.4229	4403.73978	G
4	21391.4996	-5.84454	4203.56979	NF
5	22823.82708	-5.0038	5622.552608	G

The results were not as narrow as those shown in Figure 12. The mean shear strength was lower, 4970 N, and the standard deviation was larger, 644 N. Figure 13 is a scatter plot of the shear strength results of this test.

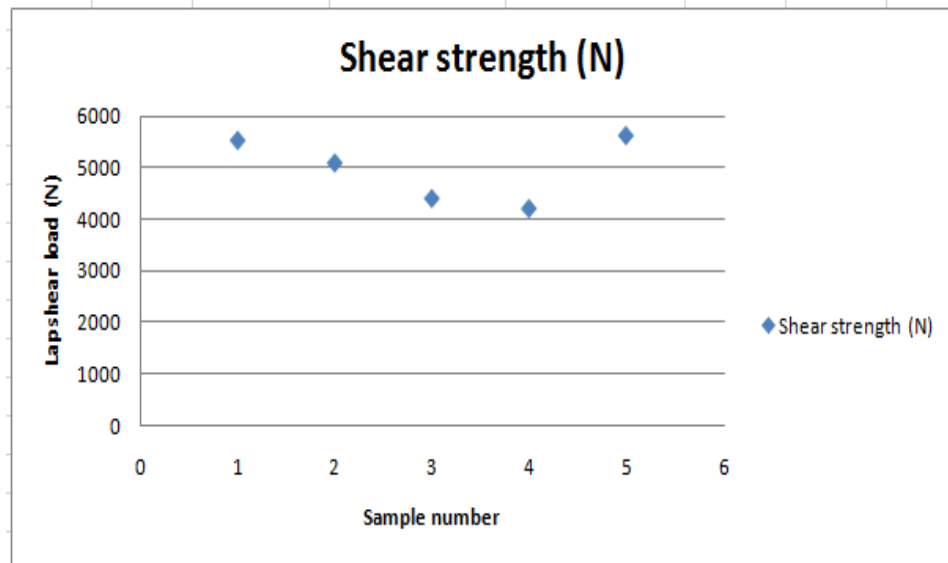


Figure 13 DP 980 fast cycle strengths

Before plunging into a formal DOE, some further preliminary small studies were advisable. One aspect of the project, with an eye to future production usage, was further reduction of cycle time. In order to be competitive with other processes that can join the same materials, the cycle time must be kept as short as possible. It was proposed that welding dwell

time be eliminated. In addition to potentially reducing cycle time, it was suggested that this would also give improved welds. Another short five-sample study was performed to test whether this concept would be useful in developing the working parameters for the Mg/steel joints, using the controller settings shown in Table 10.

Table 10 Settings without weld dwell

	Cutting	Welding	Cooling
RPM	1400	1900	0
Plunge (mm/min)	254	203.2	0
Depth (mm)	-1.524	-3.556	-3.556
Dwell (ms)	0	0	1000

The results of testing the cycle without the welding dwell time, shown in Table 11, were not encouraging.

Table 11 Results without weld dwell

Run Order	Max force (N)	Max depth (mm)	Shear force (N)	Code	Comments
1	25608.41405	-4.18846	2802.37986	G	Bit failed
2	24709.87321	-4.064	0	NJ	coated and flared bit
3	27516.70129	-4.86918	5044.283748	G	tore mg
4	25145.79897	-4.32816	4341.464672	G	tore mg
5	23402.09594	-4.11226	3545.232934	G	bit failed

Although most of the joints were good, the strengths were too wide-ranging to continue to pursue this option, as shown in Figure 14.

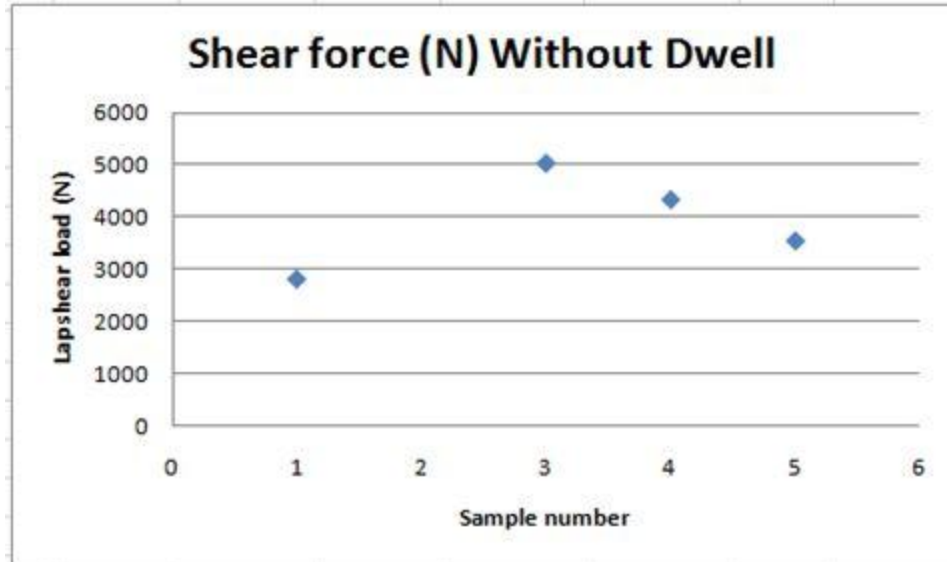


Figure 14 Strengths without weld dwell

The average was only 3933 N, with a standard deviation of 971 N. Although it is possible that future research will find a way to eliminate the welding dwell time from the FBJ cycle, at this time it is not a practical route to pursue for joining of magnesium alloys to steel.

4.5 Cross-tension and t-peel

With the “fast-cycle” settings as outlined in Table 7 being the best set of parameters found so far for the joints, cross-tension and T-peel tests (see Figure 15) were performed at those parameters, using both DP 980 and DP 590 as substrates.

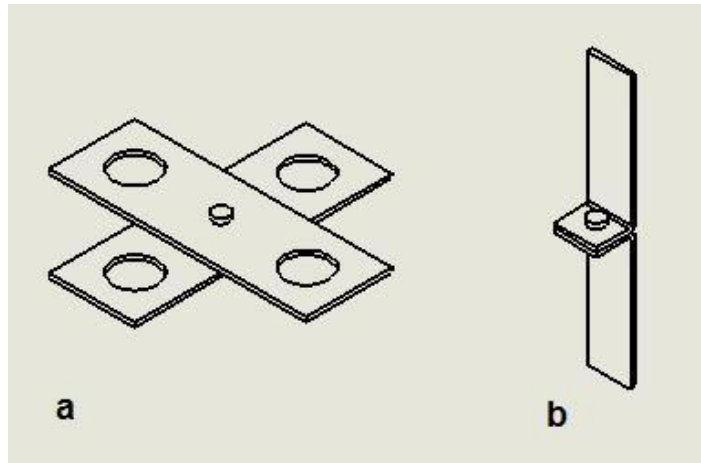


Figure 15 a) cross-tension, b) t-peel

These samples, five in each configuration with each type of steel, were made once again using the cycle parameters as shown in Table 7. However, due to errors in setup, data for only four samples was available for some sets. The results for both steels are shown in Figure 16.

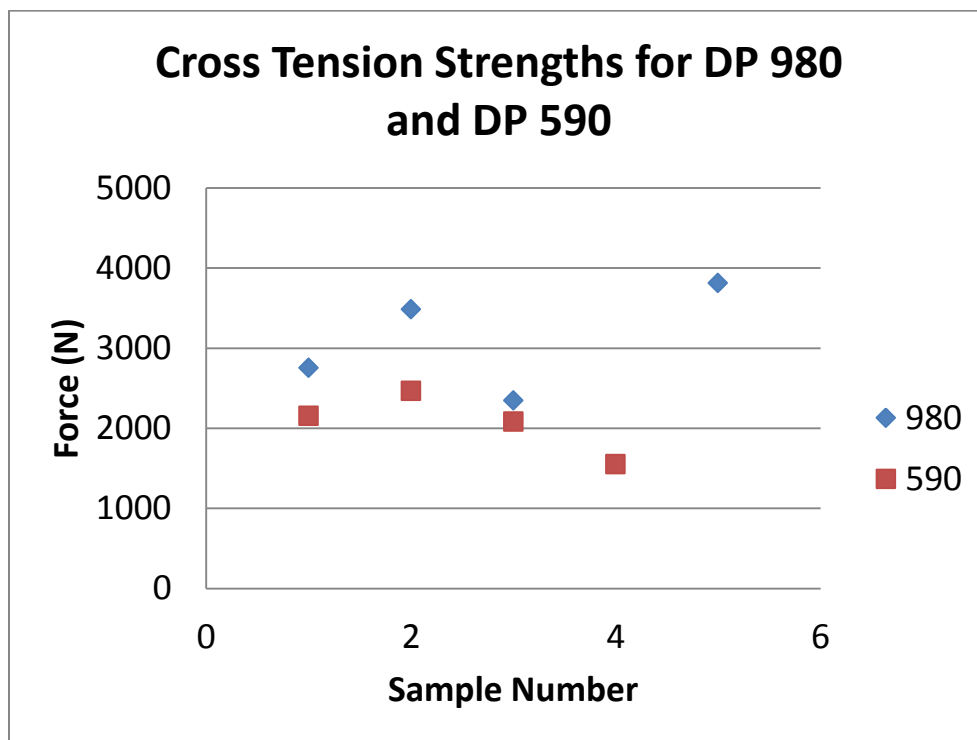


Figure 16 Cross tension results

The DP 980 cross-tension samples had an average strength of 3098 N, with a standard deviation of 670 N. The DP 590 cross-tension samples had an average strength of 2063 N, with a standard deviation of 379 N.

The t-peel tests yielded an average strength of 647 N for the DP 980, with a standard deviation of 88 N, and 514 N for the DP590, with a standard deviation of 70 N. The results of the t-peel configuration are shown in Figure 17.

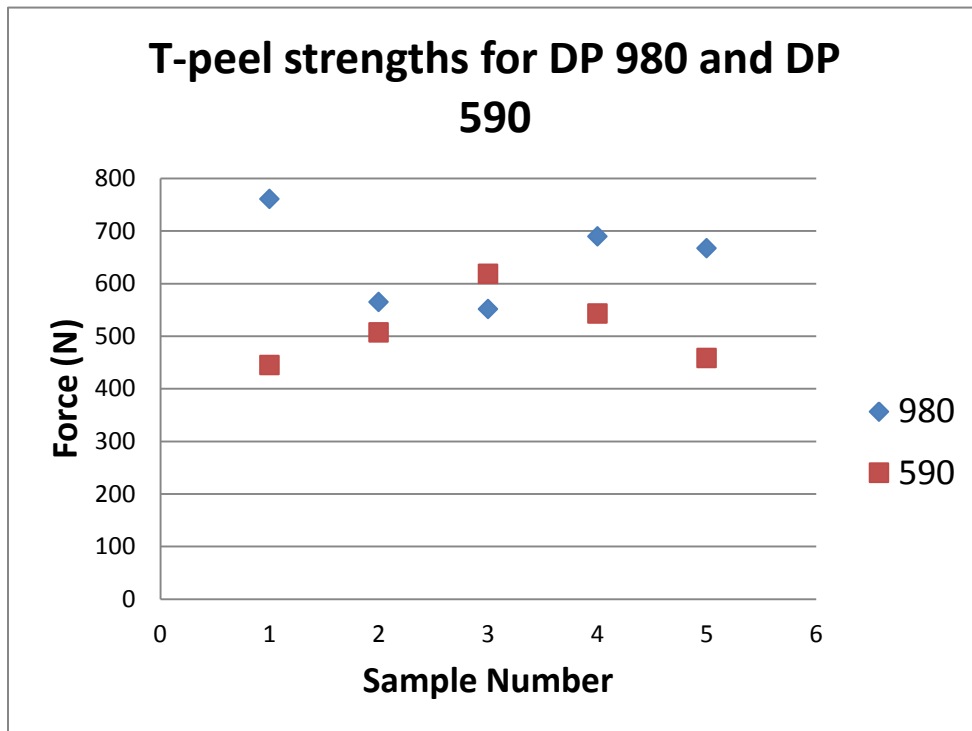


Figure 17 T-peel results

4.6 Depth study

In addition to analyzing the strength of FBJ joints, it was desirable to visually observe the joints. In order to do so, sample joints were made at three depths, cross-sectioned using a wire EDM, then sent out to be mounted, polished, and photographed. All parameters were kept

consistent except for the welding/cooling depth (shown as ‘x’ on Table 12), which was incrementally increased.

Table 12 Depth study parameters

	Cutting	Welding	Cooling
RPM	1200	2160	0
Plunge (mm/s)	4.23	4.23	0
Depth (mm)	-2.29	x	x
Dwell (ms)	0	500	500

Six samples were run, spanning a range larger than what was expected to make successful joints. The ‘x’ input depths and machine read-outs are shown in Table 13.

Table 13 Depth study data

Label	x (mm)	Force (N)	Depth (mm)	Code
	2.79	14149.09	-3.18	NJ
	3.05	16159.58	-3.68	NJ
A	3.30	16017.25	-4.31	G
B	3.56	16822.34	-4.57	G
C	3.81	16190.72	-4.91	G
	4.32	15803.74	-6.05	NJ

As expected, the more extreme depths did not result in good joints. The good samples were cut, mounted, and polished. The cross-sectional images are shown as Figure 18, Figure 19, and Figure 20.

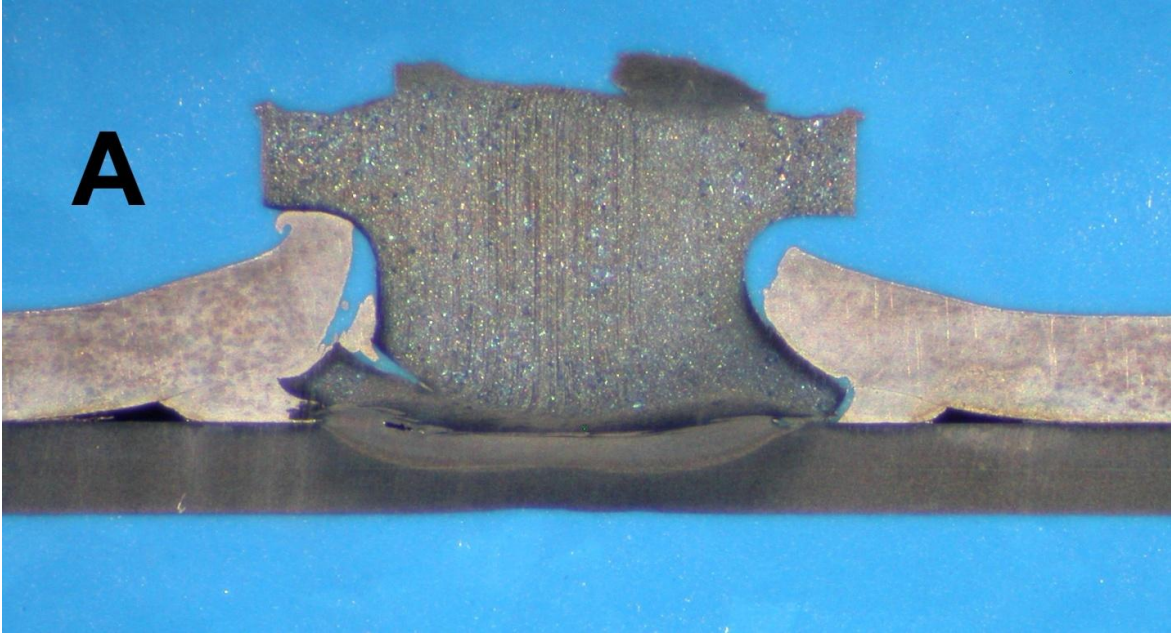


Figure 18 Sample A, nominal welding depth 3.3 mm

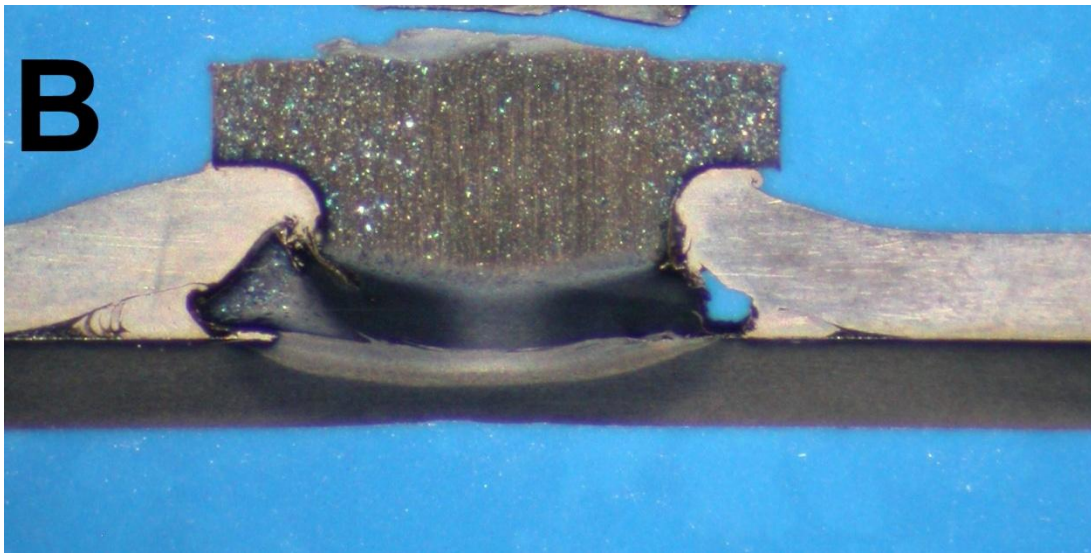


Figure 19 Sample B, nominal welding depth 3.56 mm

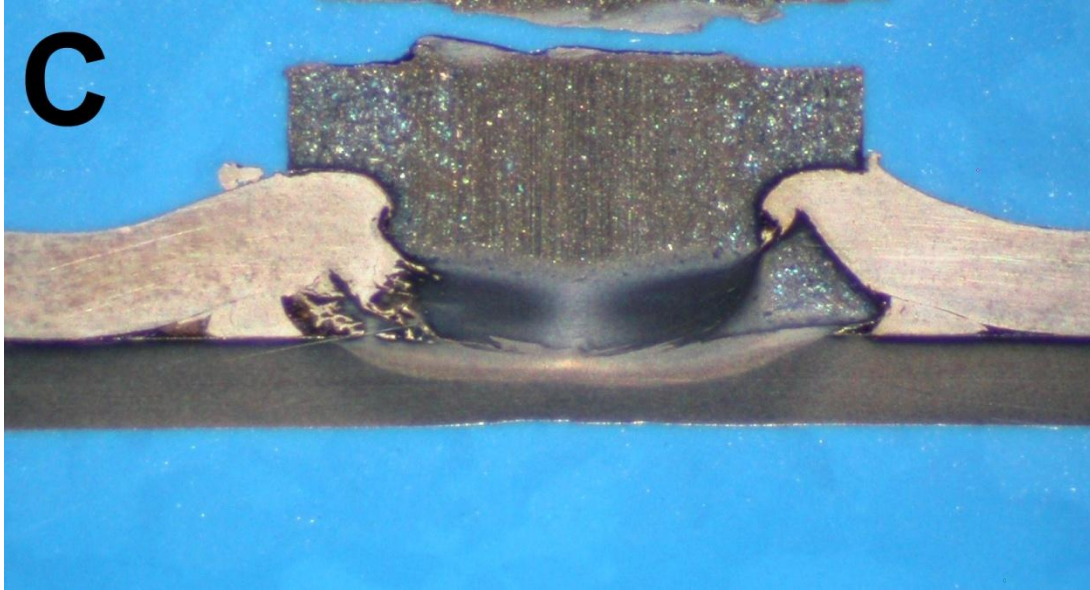


Figure 20 Sample C, nominal welding depth 3.81 mm

It is interesting to note that, even with the use of the fluted bits, the magnesium chips were not completely cleared from the joint area. In each of the three samples, it is easy to see where the chips melted cooled between the coupons. However, this pooling effect around the edges did not prevent successful joints. Another notable point is that as welding depth increased, gaps decreased. This supports the observation that stronger joints are made at increased depths. However, there is a limit to how deep the joints can be made, as was shown by the inability to make a good weld at the greatest depth tested in this experiment.

4.7 DOE

Using the data to this point as a basis for cycle parameters likely to yield successful welds, a DOE was performed to identify significant factors and interactions, and to identify the optimum combination of settings when using 4140 for the bits and DP980 as the bottom layer.

The design was a five factor full factorial with three replications, fully randomized. The factor levels are shown in Table 14.

Table 14 DOE factor levels

Factor		Low (-1)	High (+1)
Cut depth (mm)	A	-2.032	-2.54
Weld depth (mm)	B	-3.302	-4.064
Cut speed (rpm)	C	1200	1600
Weld speed (rpm)	D	2000	2500
Weld dwell (ms)	E	250	750

The full chart of controller parameters used for this experiment, including those kept constant, is shown in Table 15.

Table 15 DOE parameters

	Cutting	Welding	Cooling
RPM	C	D	0
Plunge (mm/s)	4.233	3.3864	0
Depth (mm)	A	B	B
Dwell (ms)	0	E	500

The full table of results, including factor levels and observed results, is displayed sorted by run order in Appendix C. The analysis spreadsheet, with effects and levels of significance calculated, is included as Appendix D. Effects were calculated up through three-factor interactions, although such interactions are considered to be rare. Figure 21 is a Pareto chart for visually identifying the significant effects.

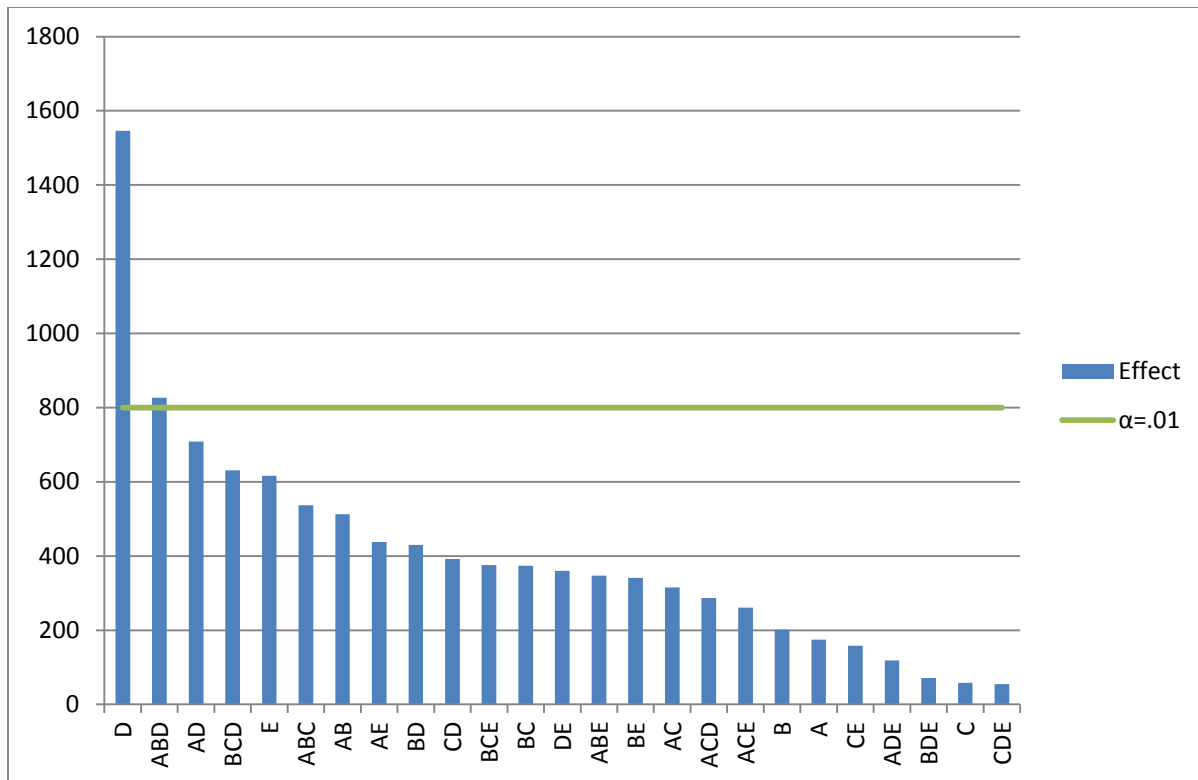


Figure 21 Pareto chart with significance calculated at $\alpha=.01$

The significant effects were D and ABD. This shows that the only factors that are not shown to influence joint strength are the cutting speed (factor C) and the weld dwell time (factor E). While it is unusual to see a significant three-way interaction, this effect cannot be disregarded, as this was a full factorial without confounding. Within the limits of this experiment, maximum joint strength is expected to occur at a cut depth of -2.03 mm, weld depth of -3.30 mm, and welding speed 2500 rpm. These settings are predicted to yield strengths averaging 5414 N when using 4140 bits to join A231 magnesium alloy to DP980 steel.

Chapter 5. Conclusions

5.1 Summary of work

Prior to the beginning of this work, FBJ had been established as capable of joining steels and steel to aluminum, but little work had been done on Mg/steel joints. Starting with the previous work as a basis, functional parameters were identified. Through iterative experimentation culminating in a multi-factor designed experiment, best parameters within the laboratory setting were identified.

5.2 Conclusions

In order to develop the FBJ process for use with magnesium alloys, this research has focused on finding optimum parameters. Within the limits of the study, optimization has been defined by shear strength and cycle time, as stated in the hypotheses.

1. The FBJ process can successfully join magnesium alloys to steel alloys with a lap shear strength in excess of 4448 N, using Self Piercing Riveting (SPR) as a benchmark for comparison. Using the settings determined by the DOE, it was shown that the process is capable of creating joints with a shear strength of 5414 N when 4140 bits to join AZ31 magnesium alloy to DP980 steel. Therefore, the hypothesis has failed to be rejected. The primary failure mode identified in lap-shear testing was fracture in the magnesium. This indicates that the strength of a good joint is limited by the properties of the magnesium layer.

2. The FBJ process time for joining magnesium alloys to steel alloys will be 2 seconds or less. Because welding dwell time was not shown to be a significant factor in the DOE, the hypothesis failed to be rejected. The plunge time and cooling time are less than or equal to 2 seconds. It should be noted that this cycle time is for the joining process only and does not include setup and removal times between joints.

5.3 Recommendations

Although the experiments have produced a set of parameters capable of meeting the stated requirements, there are further improvements that should be made. It should be noted that, in almost every instance, the recorded actual depth was greater than the nominal depth used by the machine to control the welding cycle. As the cutting and welding depths were shown to be significant factors, this is an area of concern. Further tests should be done on a machine with more accurate and precise controls (perhaps using an encoder in place of the laser micrometer for depth control). These tests should determine whether the actual best parameters should be the recorded depths from previous studies, such as this one, or if an offset of some sort is necessary for the computer input. It is to be expected that a machine which controlled the movement to only the nominal depths would not make good joints using the parameters provided here.

As all of the experiments discussed in this work were performed using AZ31 magnesium alloy, it would be of interest for additional work to be done using other magnesium alloys. It is possible that using different alloys for the upper layer of the joint could require different parameters, particularly in the cutting part of the cycle. In a related vein, further work should also determine parameters for joining magnesium alloys to magnesium alloys. Although it was outside of the limits of this study and was therefore not discussed, some attempts were made by

this researcher to complete such joints, all of which failed. However, it still seems likely that if a satisfactory bit material could be identified, parameters for successful Mg/Mg FBJ joints could be developed.

One fault of the current bit design is the changeover time. The bit is fastened into the toolholder by tightening a set screw against a flat ground onto the shank. This portion of the set-up takes several times longer than the actual welding cycle. As this non-value-added time is not efficient for production use, it is suggested that another bit design be developed that would allow for faster changeover. If the improved bit design could eliminate the shank, this would also cut down on waste.

With further improvements to the bit design, material which can be joined, and overall reliability of the process, it is expected that FBJ will be able to take its place in production-level spot joining methods. FBJ has been shown to be capable of joining materials difficult to join using conventional methods, including magnesium alloys and ultra high strength steels. Further research and developments will lead to better understanding and applications of the FBJ process.

References

- Borrisutthekul, R., Y. Miyashita, and Y. Mutoh. "Dissimilar material laser welding between magnesium alloy AZ31B and aluminum alloy A5052-O." *Science and Technology of Advanced materials* 6, no. 2: 199-204.
- Chen, Y. K., L. Han, A. Chrysanthou, and J. M. O'Sullivan. "Fretting wear in self-piercing riveted aluminium alloy sheet." *Wear* 255, no. 7-12: 1463-1470.
- Cole, G. S., and A. M. Sherman. "Lightweight Materials for Automotive Applications." *Materials Characterization*, 1995: 3-9.
- Fu, M., and P. K. Mallick. "Fatigue of self-piercing riveted joints in aluminum alloy 6111." *International Journal of Fatigue* 25, no. 3 (2003): 183-189.
- Gerlich, A., P. Su, and T. H. North. "Peak temperatures and microstructures in aluminium and magnesium alloy friction stir spot welds." *Science and Technology of Welding and Joining* 10, no. 6 (2005): 647-652.
- He, X., I. Pearson, and K. Young. "Self-pierce riveting for sheet materials: State of the art." *Journal of Materials Processing Technology* 199, no. 1-3 (2008): 27-36.
- Kwon, Y. J., I. Shigematsu, and N. Saito. "Dissimilar friction stir welding between magnesium and aluminum alloys." *Materials Letters* 62, no. 23: 3827-3829.
- Miles, M. P., K. Kohkonen, S. Packer, R. Steel, B. Siemssen, and Y. S. Sato. "Solid state spot joining of sheet materials using consumable bit." *Science and Technology of Welding and Joining* 14 (2009): 72-77.
- Neugebauer, R., S. Dietrich, and C. Kraus. "Dieless clinching and dieless rivet-clinching of magnesium." *Key Engineering Materials* 344 (2007): 693-698.
- Ochi, H., K. Ogawa, Y. Yamamoto, G. Kawai, R. Tsujino, and Y. Suga. "Effect of intermetallic compounds on friction weldability of aluminum alloys to S25C carbon steel." *Zairyo/Journal of the Society of Materials Science* 53, no. 5 (2004): 532-538.
- Pan, T., W. J. Schwartz, and K. A. Lazarz. "Spot Friction Weldbonding for sheet aluminum joining, paper 17." (Ford Research and Advanced Engineering, Ford Motor Company).

- Quan, Y., and etal. "CO2 Laser Beam welding of Dissimilar magnesium-Based Alloys." *Materials Science and Engineering: A* 496, no. 1-2: 45-51.
- Satyanarayana, V. V., G. Madhusudhan Reddy, and T. Mohandas. "Dissimilar metal friction welding of austenitic-ferritic stainless steels." *Journal of Materials Processing Technology* 160, no. 2 (2005): 128-137.
- Song, G., L. Liming, and W. Peichong. "Overlap welding of magnesium AZ31B sheets using laser-arc hybrid process." *Materials Science & Engineering A*, 2006: 312-319.
- Sun, D. Q., B. Lang, D. X. Sun, and J. B. Li. "Microstructures and mechanical properties of resistance spot welded magnesium alloy joints." *Material Science and Engineering A*, 2007: 494-498.
- Yamamoto, M., A. Gerlich, T. H. North, and K. Shinozaki. "Cracking in dissimilar Mg alloy friction stir spot welds." *Science and Technology of Welding and Joining* 13, no. 7 (2008): 583-592.

Appendix A Glossary of terms

Chips	Material removed in cutting processes.
Cross-tension	A joint configuration in which the joined area is in the center of two materials oriented at 90 degrees to each other. In testing, the materials are bolted to the test fixture so that the joint is in tension.
DOE	Design of Experiments, a statistical methodology enabling the testing and analysis of multiple factors, or variables, simultaneously
FBJ	Friction Bit Joining, a spot joining technology in which a consumable bit cuts through an upper layer and friction-welds to a lower layer.
Flute	A recess or channel cut into a tool to allow for removal of material which has been cut away.

FSSW	Friction Stir Spot Welding, a spot joining technology in which a non-consumable tool is rapidly rotated and plunged into overlapping materials. The friction between the tool and the metals softens the metals and stirs them together, causing a dimpled weld to remain when the tool is retracted.
FSW	Friction Stir Welding, a joining technology in which a non-consumable tool is rapidly rotated and plunged into butted or overlapping materials. The friction between the tool and the materials to be joined softens the materials and stirs them together.
FW	Friction Welding, a joining process using the heat caused by friction between two materials to cause a joint.
Lap shear	A joint configuration in which parallel materials being joined overlap at the joint location. When the materials are placed in tension, shear forces are induced across the joint.
Mg	Chemical symbol for magnesium. For the purposes of this paper, the symbol is also used to refer to magnesium alloys, as pure magnesium was never used in the research.
RPM	Rotations per minute

RSW	Resistance Spot Welding, a spot joining technology in which metals to be joined are clamped between two electrodes. The heat generated by the resistance in the metals causes the materials to weld together.
SPR	Self-Piercing Riveting, a mechanical spot joining technology in which a consumable rivet pierces the metals being joined and flares out, holding the metals together.
T-peel	A joint configuration in which the joined area is at a 90 degree angle to the remainder of the material. The two materials are, in turn, at 180 degrees from each other. When the materials are placed in tension, the joint is 'peeled' apart at failure.
UHSS	Ultra High Strength Steel

Appendix B Machine code for fluted bits

```
$STELMAG2.MIN%
DEF WORK
PS LC,[-15,0],[15,05]
END
DRAW
G00 X20 Z20
G50 S2500
X.40 Z.1 S1000 T010101 M03 M42 M08 (TOOL 1)
G96 S400
G85 NLAP1 D.05 F.005 U.015 W.004 (ROUGH CUT)
NLAP1 G81 (DEFINE PROFILE)
G00 X0
G01 Z0 G42 F.003
X.215
G76 X.235 Z-.193 L.060
X.375
Z-.408
X.3125 Z-.508
Z-1.25
X.375
G40 X.40
G80
G00 Z.1
G96 S450
G87 NLAP1 (FINISH CUT)
G00 Z.1
G97 S1000
X20 Z20
X.45 Z-.458 S1000 T040404 M03 M08 (TOOL CHANGE – 1/8 INCH SQUARE GROOVE)
G97 S1000
G73 X.308 Z-.508 K.1 D.5 L.5 F.003
G00 Z.1M9
G97 S1000
X20 Z20
X.50 Z-.278 S1000 T030303 M03 M08 (TOOL CHANGE – 1/16 MODIFIED GROOVE)
G97 S1000
```

```

G73 X.212 Z-.278 K0 D.03 L.06 F.002
G00 Z.1
N500 G00 X20 Z20 M05
M110 (C-AXIS JOINT)
M146 M15 (C-AXIS UNCLAMP)
(START GROOVING AND SHAPING HEAD)
G00 X20 Z20 M05
M110
M15
G94 X.75 Z.3 T1212 SB=2000 M13 M08
X.45 Z.05
G190 X.165 Z-.070 C0 K.060 D.05 W.015 E8.0 F3.0 M211 M213 (GROOVE HEAD)
C180
G180
G00 X20 Z20 M12 M146
G95 M109
M05
M110
M16
G95 X.35 Z.4 T0606 SB=1200 M13
Z.065
G185 X.012 Z.015 C0 F.100 SA=4.0 (CUT TAPERS ON SIDES OF HEAD)
G180
G00 X.35 Z.4
C180
Z.065
G185 X.012 Z.015 C180 F.100 SA=4.0
G180
G00 X20 Z20 M12 M146
G95 M109 (FEED IN/REV – CANCEL M110)
G97 S1000 M03
G00 X20 Z20 (HOME)
X.45 Z-1.25 S1000 T080808 M03 M08 TOOL CHANGE – PARTING TOOL)
G97 S1200
G01 X.25 F.00 (BEGIN PART OFF)
G00 X.314 (REPOSITION)
Z-1.20 (REPOSITION)
G01 X.25 Z-1.25 (CUT ANGLE)
X0 (FINISH PART OFF)
G00 X.45
X20 Z20
M02
%
```

Appendix C DOE recorded data

Design Order	Run Order	cut depth	weld depth	cut speed	weld speed	dwll time	Max Force	Max Depth	Strength	Code
78	1	2.032	4.064	1600	2000	250	15617.71	89179.4	4537.19	G
94	2	2.54	4.064	1600	2000	250	16520.7	94335.6	0.00	NJ
52	3	2.54	3.302	1200	2500	250	13104.46	74828.4	5422.38	G
33	4	2.032	3.302	1200	2000	750	15862.36	90576.4	0.00	NJ
65	5	2.032	3.302	1200	2000	750	17392.55	99314	1147.64	NF
62	6	2.54	4.064	1600	2000	250	16098.12	91922.6	1116.50	NF
64	7	2.54	4.064	1600	2500	250	18095.37	103327.2	5351.21	G
59	8	2.54	4.064	1200	2500	750	15390.85	87884	4866.35	G
73	9	2.032	4.064	1200	2000	750	16569.63	94615	4434.88	G
96	10	2.54	4.064	1600	2500	250	16929.93	96672.4	1249.95	NF
37	11	2.032	3.302	1600	2000	750	17036.69	97282	3843.26	G
63	12	2.54	4.064	1600	2500	750	13656.04	77978	4328.12	G
9	13	2.032	4.064	1200	2000	750	19354.21	110515.4	3095.96	NF
24	14	2.54	3.302	1600	2500	250	14474.51	82651.6	1934.98	G
48	15	2.032	4.064	1600	2500	250	15724.46	89789	3972.26	G
34	16	2.032	3.302	1200	2000	250	16151.49	92227.4	511.55	NF
76	17	2.032	4.064	1200	2500	250	14443.38	82473.8	4995.35	G
3	18	2.032	3.302	1200	2500	750	15039.44	85877.4	4603.91	G
20	19	2.54	3.302	1200	2500	250	14648	83642.2	4719.56	G
1	20	2.032	3.302	1200	2000	750	18215.47	104013	4968.66	G
45	21	2.032	4.064	1600	2000	750	15252.95	87096.6	1156.54	NF
56	22	2.54	3.302	1600	2500	250	14301.03	81661	4795.18	G
86	23	2.54	3.302	1600	2000	250	18882.7	107823	4248.05	G

Design Order	Run Order	cut depth	weld depth	cut speed	weld speed	dwll time	Max Force	Max Depth	Strength	Code
66	24	2.032	3.302	1200	2000	250	16418.39	93751.4	1040.88	NF
29	25	2.54	4.064	1600	2000	750	17503.75	99949	716.16	NF
68	26	2.032	3.302	1200	2500	250	15937.98	91008.2	5667.03	G
4	27	2.032	3.302	1200	2500	250	15800.08	90220.8	2837.97	G
7	28	2.032	3.302	1600	2500	750	14283.24	81559.4	3367.30	NF
79	29	2.032	4.064	1600	2500	750	14194.28	81051.4	5151.04	G
21	30	2.54	3.302	1600	2000	750	18789.29	107289.6	4443.77	G
14	31	2.032	4.064	1600	2000	250	16338.32	93294.2	1708.12	NF
19	32	2.54	3.302	1200	2500	750	17410.34	99415.6	2428.73	NF
55	33	2.54	3.302	1600	2500	750	13918.49	79476.6	1098.71	NF
90	34	2.54	4.064	1200	2000	250	19109.56	109118.4	2032.84	NF
44	35	2.032	4.064	1200	2500	250	15066.13	86029.8	4941.97	G
87	36	2.54	3.302	1600	2500	750	17076.72	97510.6	4964.22	G
43	37	2.032	4.064	1200	2500	750	15813.43	90297	4875.25	G
40	38	2.032	3.302	1600	2500	250	14825.92	84658.2	4728.46	G
93	39	2.54	4.064	1600	2000	750	17259.1	98552	1267.74	NF
22	40	2.54	3.302	1600	2000	250	17130.1	97815.4	4034.54	G
35	41	2.032	3.302	1200	2500	750	16342.77	93319.6	5377.90	G
15	42	2.032	4.064	1600	2500	750	16645.25	95046.8	5128.80	G
27	43	2.54	4.064	1200	2500	750	14341.07	81889.6	5093.21	G
71	44	2.032	3.302	1600	2500	750	14874.85	84937.6	4888.60	G
38	45	2.032	3.302	1600	2000	250	21516.05	122859.8	991.95	NF
17	46	2.54	3.302	1200	2000	750	18219.92	104038.4	4959.77	G
41	47	2.032	4.064	1200	2000	750	17098.97	97637.6	796.23	NF
92	48	2.54	4.064	1200	2500	250	18340.02	104724.2	1169.88	NF
75	49	2.032	4.064	1200	2500	750	16614.11	94869	5342.31	G
67	50	2.032	3.302	1200	2500	750	15101.71	86233	5644.79	G
83	51	2.54	3.302	1200	2500	750	15800.08	90220.8	1432.33	NF
46	52	2.032	4.064	1600	2000	250	17392.55	99314	1387.85	NF

Design Order	Run Order	cut depth	weld depth	cut speed	weld speed	dwll time	Max Force	Max Depth	Strength	Code
77	53	2.032	4.064	1600	2000	750	16938.83	96723.2	4546.08	G
60	54	2.54	4.064	1200	2500	250	16338.32	93294.2	2909.14	NF
89	55	2.54	4.064	1200	2000	750	17245.76	98475.8	5106.56	G
80	56	2.032	4.064	1600	2500	250	14465.62	82600.8	5311.18	G
82	57	2.54	3.302	1200	2000	250	17219.07	98323.4	4074.57	G
12	58	2.032	4.064	1200	2500	250	13793.94	78765.4	4790.74	G
57	59	2.54	4.064	1200	2000	750	17156.79	97967.8	4612.81	G
54	60	2.54	3.302	1600	2000	250	17001.1	97078.8	4941.97	G
50	61	2.54	3.302	1200	2000	250	17632.75	100685.6	0.00	NJ
61	62	2.54	4.064	1600	2000	750	17944.13	102463.6	2144.04	NF
74	63	2.032	4.064	1200	2000	250	19127.35	109220	760.65	NF
31	64	2.54	4.064	1600	2500	750	15110.61	86283.8	4554.98	G
11	65	2.032	4.064	1200	2500	750	15969.12	91186	5097.66	G
18	66	2.54	3.302	1200	2000	250	17241.31	98450.4	0.00	NJ
70	67	2.032	3.302	1600	2000	250	17379.2	99237.8	2068.42	NF
10	68	2.032	4.064	1200	2000	250	17948.58	102489	787.34	NF
84	69	2.54	3.302	1200	2500	250	16409.49	93700.6	1040.88	NF
49	70	2.54	3.302	1200	2000	750	20052.58	114503.2	4479.36	G
53	71	2.54	3.302	1600	2000	750	17539.34	100152.2	5453.52	G
23	72	2.54	3.302	1600	2500	750	13442.53	76758.8	3216.06	NF
30	73	2.54	4.064	1600	2000	250	18357.81	104825.8	1036.44	NF
6	74	2.032	3.302	1600	2000	250	16542.94	94462.6	0.00	NJ
36	75	2.032	3.302	1200	2500	250	14367.76	82042	5297.83	G
26	76	2.54	4.064	1200	2000	250	17125.65	97790	1036.44	NF
8	77	2.032	3.302	1600	2500	250	15083.92	86131.4	1307.78	NF
28	78	2.54	4.064	1200	2500	250	15519.85	88620.6	3950.02	G
85	79	2.54	3.302	1600	2000	750	20306.13	115951	5284.49	G
39	80	2.032	3.302	1600	2500	750	14034.14	80137	2277.49	NF
69	81	2.032	3.302	1600	2000	750	14968.27	85471	0.00	NJ

Design Order	Run Order	cut depth	weld depth	cut speed	weld speed	dwll time	Max Force	Max Depth	Strength	Code
91	82	2.54	4.064	1200	2500	750	15097.27	86207.6	4768.49	G
16	83	2.032	4.064	1600	2500	250	12125.85	69240.4	4425.98	G
47	84	2.032	4.064	1600	2500	750	15373.06	87782.4	1027.54	NJ
5	85	2.032	3.302	1600	2000	750	16760.9	95707.2	3398.44	NF
88	86	2.54	3.302	1600	2500	250	14118.66	80619.6	2001.70	G
51	87	2.54	3.302	1200	2500	750	15853.46	90525.6	3843.26	NF
72	88	2.032	3.302	1600	2500	250	12753.05	72821.8	5257.80	G
81	89	2.54	3.302	1200	2000	750	11431.93	65278	0.00	NJ
42	90	2.032	4.064	1200	2000	250	16195.98	92481.4	5257.80	G
95	91	2.54	4.064	1600	2500	750	14314.38	81737.2	2362.01	NF
32	92	2.54	4.064	1600	2500	250	14345.52	81915	4563.88	G
25	93	2.54	4.064	1200	2000	750	17592.72	100457	3233.86	NF
2	94	2.032	3.302	1200	2000	250	18411.19	105130.6	4523.84	G
13	95	2.032	4.064	1600	2000	750	17606.06	100533.2	4296.98	G
58	96	2.54	4.064	1200	2000	250	16293.84	93040.2	800.68	NF

Appendix D DOE analysis

	A	B	C	D	E	AB	AC	AD	AE	BC	BD	BE	CD	CE	DE	ABC	ABD	ABE	ACD	ACE	ADE	BCD	BCE	BDE	CDE	Year	V _{eff}					
1	-1	-1	-1	-1	-1	-1	-1	-1	-1	-1	-1	-1	-1	-1	-1	-1	-1	-1	-1	-1	-1	-1	-1	-1	-1	458.3333	342022.3					
2	-1	-1	-1	-1	-1	-1	-1	-1	-1	-1	-1	-1	-1	-1	-1	-1	-1	-1	-1	-1	-1	-1	-1	-1	-1	-1	455.3333	240142.3				
3	-1	-1	-1	-1	-1	-1	-1	-1	-1	-1	-1	-1	-1	-1	-1	-1	-1	-1	-1	-1	-1	-1	-1	-1	-1	-1	1171	14772				
4	-1	-1	-1	-1	-1	-1	-1	-1	-1	-1	-1	-1	-1	-1	-1	-1	-1	-1	-1	-1	-1	-1	-1	-1	-1	-1	1034.333	119332.3				
5	-1	-1	-1	-1	-1	-1	-1	-1	-1	-1	-1	-1	-1	-1	-1	-1	-1	-1	-1	-1	-1	-1	-1	-1	-1	-1	542.6667	223305.3				
6	-1	-1	-1	-1	-1	-1	-1	-1	-1	-1	-1	-1	-1	-1	-1	-1	-1	-1	-1	-1	-1	-1	-1	-1	-1	-1	229.3333	54086.33				
7	-1	-1	-1	-1	-1	-1	-1	-1	-1	-1	-1	-1	-1	-1	-1	-1	-1	-1	-1	-1	-1	-1	-1	-1	-1	-1	789.3333	89506.33				
8	-1	-1	-1	-1	-1	-1	-1	-1	-1	-1	-1	-1	-1	-1	-1	-1	-1	-1	-1	-1	-1	-1	-1	-1	-1	-1	846.3333	221444.3				
9	-1	-1	-1	-1	-1	-1	-1	-1	-1	-1	-1	-1	-1	-1	-1	-1	-1	-1	-1	-1	-1	-1	-1	-1	-1	-1	624	171169				
10	-1	-1	-1	-1	-1	-1	-1	-1	-1	-1	-1	-1	-1	-1	-1	-1	-1	-1	-1	-1	-1	-1	-1	-1	-1	-1	510	388997				
11	-1	-1	-1	-1	-1	-1	-1	-1	-1	-1	-1	-1	-1	-1	-1	-1	-1	-1	-1	-1	-1	-1	-1	-1	-1	-1	1147.667	228333				
12	-1	-1	-1	-1	-1	-1	-1	-1	-1	-1	-1	-1	-1	-1	-1	-1	-1	-1	-1	-1	-1	-1	-1	-1	-1	-1	1103.667	895333				
13	-1	-1	-1	-1	-1	-1	-1	-1	-1	-1	-1	-1	-1	-1	-1	-1	-1	-1	-1	-1	-1	-1	-1	-1	-1	-1	749.3333	151822				
14	-1	-1	-1	-1	-1	-1	-1	-1	-1	-1	-1	-1	-1	-1	-1	-1	-1	-1	-1	-1	-1	-1	-1	-1	-1	-1	579	151822				
15	-1	-1	-1	-1	-1	-1	-1	-1	-1	-1	-1	-1	-1	-1	-1	-1	-1	-1	-1	-1	-1	-1	-1	-1	-1	-1	847.3333	846906.3				
16	-1	-1	-1	-1	-1	-1	-1	-1	-1	-1	-1	-1	-1	-1	-1	-1	-1	-1	-1	-1	-1	-1	-1	-1	-1	-1	1027.333	24444.33				
17	-1	-1	-1	-1	-1	-1	-1	-1	-1	-1	-1	-1	-1	-1	-1	-1	-1	-1	-1	-1	-1	-1	-1	-1	-1	-1	728.6667	194892.3				
18	-1	-1	-1	-1	-1	-1	-1	-1	-1	-1	-1	-1	-1	-1	-1	-1	-1	-1	-1	-1	-1	-1	-1	-1	-1	-1	805.3333	278156.3				
19	-1	-1	-1	-1	-1	-1	-1	-1	-1	-1	-1	-1	-1	-1	-1	-1	-1	-1	-1	-1	-1	-1	-1	-1	-1	-1	707.3333	278156.3				
20	-1	-1	-1	-1	-1	-1	-1	-1	-1	-1	-1	-1	-1	-1	-1	-1	-1	-1	-1	-1	-1	-1	-1	-1	-1	-1	577.3333	74177.33				
21	-1	-1	-1	-1	-1	-1	-1	-1	-1	-1	-1	-1	-1	-1	-1	-1	-1	-1	-1	-1	-1	-1	-1	-1	-1	-1	888	279853				
22	-1	-1	-1	-1	-1	-1	-1	-1	-1	-1	-1	-1	-1	-1	-1	-1	-1	-1	-1	-1	-1	-1	-1	-1	-1	-1	1137.667	44782.33				
23	-1	-1	-1	-1	-1	-1	-1	-1	-1	-1	-1	-1	-1	-1	-1	-1	-1	-1	-1	-1	-1	-1	-1	-1	-1	-1	991	113776				
24	-1	-1	-1	-1	-1	-1	-1	-1	-1	-1	-1	-1	-1	-1	-1	-1	-1	-1	-1	-1	-1	-1	-1	-1	-1	-1	695.3333	89364.3				
25	-1	-1	-1	-1	-1	-1	-1	-1	-1	-1	-1	-1	-1	-1	-1	-1	-1	-1	-1	-1	-1	-1	-1	-1	-1	-1	654.3333	134676.3				
26	-1	-1	-1	-1	-1	-1	-1	-1	-1	-1	-1	-1	-1	-1	-1	-1	-1	-1	-1	-1	-1	-1	-1	-1	-1	-1	970.6667	47610.33				
27	-1	-1	-1	-1	-1	-1	-1	-1	-1	-1	-1	-1	-1	-1	-1	-1	-1	-1	-1	-1	-1	-1	-1	-1	-1	-1	290	21619				
28	-1	-1	-1	-1	-1	-1	-1	-1	-1	-1	-1	-1	-1	-1	-1	-1	-1	-1	-1	-1	-1	-1	-1	-1	-1	-1	1103.667	4402.333				
29	-1	-1	-1	-1	-1	-1	-1	-1	-1	-1	-1	-1	-1	-1	-1	-1	-1	-1	-1	-1	-1	-1	-1	-1	-1	-1	601.6667	99710.33				
30	-1	-1	-1	-1	-1	-1	-1	-1	-1	-1	-1	-1	-1	-1	-1	-1	-1	-1	-1	-1	-1	-1	-1	-1	-1	-1	309.3333	86204.33				
31	-1	-1	-1	-1	-1	-1	-1	-1	-1	-1	-1	-1	-1	-1	-1	-1	-1	-1	-1	-1	-1	-1	-1	-1	-1	-1	161.3333	19602.33				
32	-1	-1	-1	-1	-1	-1	-1	-1	-1	-1	-1	-1	-1	-1	-1	-1	-1	-1	-1	-1	-1	-1	-1	-1	-1	-1	842.6667	23502.33				
ΣY _e	10964.33	11515	11180.67	12933.67	10950	10460.33	12081.33	9107.667	10398.67	10398.67	10398.67	11671	10758.67	11359.33	11883	10954.67	10076.67	12155.67	10999.33	12351.33	12027	11558.67	11473.33	11669.67	10579.33	11377.67						
ΣY _e	11949.67	11573.33	11891.67	10138.67	12122.33	12612	10994	13964.67	12673.67	12673.67	12673.67	14001.33	12313.67	11719	11089.33	12477.67	12995.67	10916.67	12073	10721	11045.33	11813.67	11599	11402.67	112493	11700.67						
Year _e	685.2708	715.6875	698.7917	808.3542	684.375	653.7708	735.0833	589.2292	648.9167	648.9167	648.9167	671.4375	671.4375	709.9383	748.9375	662.1667	629.7917	759.7292	687.4583	771.9583	751.6875	703.6667	717.0833	729.3542	661.2883	710.7292						
Year _e	728.1042	722.3333	743.2292	653.6667	757.6458	788.25	686.9375	672.7917	792.1042	779.6042	712.5833	769.6042	732.0625	693.0833	779.6542	812.2292	682.2917	754.5625	670.0625	690.3333	738.3342	724.9375	712.6667	780.8125	731.9317							
Effect	-42.8333	-2.64583	-44.4375	174.6875	-78.2708	-134.479	68.14583	-305.563	-142.188	-117.188	16.85417	-97.1875	-22.1692	55.85417	-117.688	-182.438	77.4375	-67.1042	101.8998	61.35417	-34.6875	-7.85417	16.6875	-119.604	-20.6625							
S _e	367.3611																															
S _{eff}	74.98727																															
df	64																															
t _{0.64, 0.05}	1.699																															
Decision	125.1527																															
Decision I	-178.92																															